

# Creation of simplified state-dependent fragility functions through ad-hoc scaling factors to account for previous damage in a multi-hazard risk context. An application to flow-depth-based analytical tsunami fragility functions for the Pacific coast of South America

(<https://doi.org/10.5880/riesgos.2022.002>)

---

Juan Camilo Gómez Zapata<sup>1,2</sup> Sergio Medina<sup>3</sup>, Juan Lizarazo-Marriaga<sup>3</sup>

1. Seismic Hazard and Risk Dynamics, GFZ German Research Centre for Geosciences, Potsdam, Germany
2. Institute for Geosciences, University of Potsdam, Potsdam, Germany
3. Departamento de Ingeniería Civil y Agrícola, Universidad Nacional de Colombia, Bogotá, Colombia

## 1. Licence

Creative Commons Attribution 4.0 International License (CC BY 4.0)



## 2. Citation

**When using the data please cite:**

Gomez-Zapata, J. C.; Medina, S.; Lizarazo-Marriaga, J. (2022): Creation of simplified state-dependent fragility functions through ad-hoc scaling factors to account for previous damage in a multi-hazard risk context. An application to flow-depth-based analytical tsunami fragility functions for the Pacific coast of South America. GFZ Data Services. <https://doi.org/10.5880/riesgos.2022.002>

**The data are supplementary material to:**

Gómez Zapata, J. C., Pittore, M., Brinckmann, N., Lizarazo-Marriaga, J., Medina, S., Tarque, N., & Cotton, F. (2023). Scenario-based multi-risk assessment from existing single-hazard vulnerability models. An application to consecutive earthquakes and tsunamis in Lima, Peru. In *Natural Hazards and Earth System Sciences* (Vol. 23, Issue 6, pp. 2203–2228). Copernicus GmbH. <https://doi.org/10.5194/nhess-23-2203-2023>

## Table of contents

1. Licence .....	1
2. Citation.....	1
3. Data Description .....	2
4. File description.....	2
5. Acknowledgments.....	7
6. References .....	7

### 3. Data Description

This data repository contains a brief description of the building classification scheme for physical vulnerability to tsunamis and corresponding fragility functions originally proposed by Medina, 2019. These fragility functions are used as input to construct their associated state-dependent fragility functions using scaling factors, which were obtained as ad-hoc calibration parameters. A Python script to produce a file with such a model is provided along with the needed inputs and resulting output files.

### 4. File description

The building classification scheme and their corresponding fragility functions for physical vulnerability to tsunamis originally proposed by Medina, 2019 [1] for the city of Tumaco (Colombia) was adopted in the paper for which this data repository is a supplement. The reason for this extrapolation is that this classification scheme comprises the only far-field tsunami fragility analytical functions available for the Pacific coast of South America. For its actual implementation in the study area of Metropolitan Lima (Peru), we had to reduce one class (out of the initially proposed seven building types proposed) to six typologies (since one of these typologies is exclusive to Tumaco). The remaining set comprises four types of concrete, one of wood and one of masonry.

Original figures from Medina, 2019 [1] for such generalized models of these structures are provided below. These representations allowed the author to create finite element models to then perform the nonlinear computational analysis using the OpenSees® platform [2] and derive their associated analytical fragility functions. Later, we also provide a short summary on the manner these fragility functions are derived. A more comprehensive explanation of the involved approaches and assumptions are documented in Medina et al, 2019 [3].

#### Masonry (M-MP).

This simple masonry buildings are assumed to have a small rectangular shape without reaching or exceeding 2 levels. Although they do not present reinforcing steel or reinforced concrete frames, they are assumed to have crown beams and concrete plates. Figure 1 shows a generic distribution of the structural elements of this building type. This typology has the following characteristics:

- Geometry in rectangular plan
- Height between floors of 3m
- The thickness of the walls is 12cm.
- Concrete slab thickness 10cm.

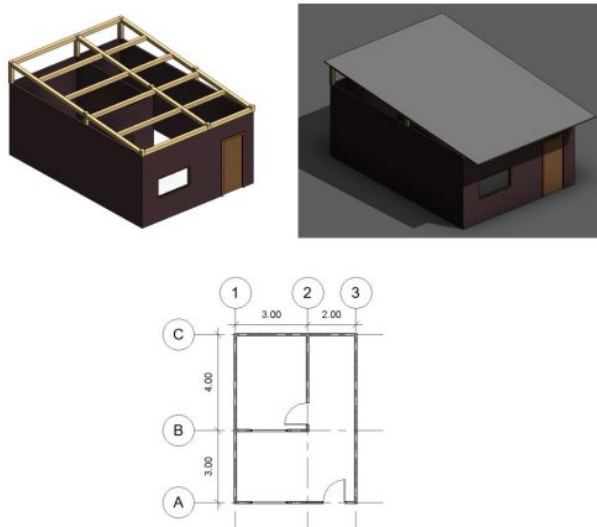


Figure 1. Schematic representation of M-M-P. Reprint from [1]

### Wood Panels (M-PN).

Its predominant geometry is rectangular in plan. Its wooden panels work as a diaphragm between frames and at the same time act as dividing walls. Figure 2 shows at the bottom shows the distribution of the structural elements of this type of dwelling. Its main characteristics are:

- Geometry in rectangular plan.
- Floor height of 3 m.
- Flexible diaphragm, for wooden floors and wooden decks.
- Slab thickness 3cm, in wood.

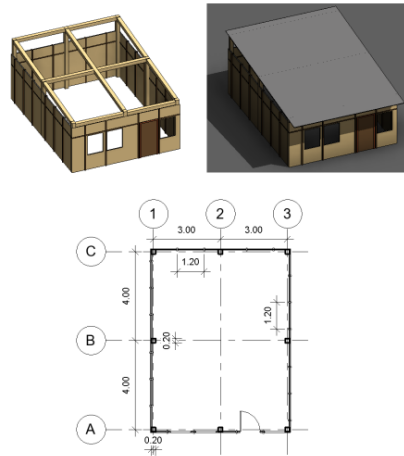


Figure 2. Schematic representation of M-PN. Reprint from [1]

**Concrete frames (M-PCP):** They are structures with enough rigidity to stand up against lateral loads, but they have enough flexibility to generate plastic hinges that allow energy to be dissipated, mainly when subjected to cyclic loads. Four types of buildings were classified as concrete frames.

### Concrete frames - 1 story (M-PCP1-T1).

It is a one (1) story structure with a width/length ratio approximately equal to 1. Figure 3 shows a generic distribution of the structural elements of this building type. Its main characteristics are:

- Rectangular geometry in plan.
- Square columns (25cm x 25cm).
- Rectangular beams (25cm x 30cm).
- Mezzanine height of 3m.
- Between its porches there are dividing walls and facades in brick blocks
- Concrete slab thickness 10cm.

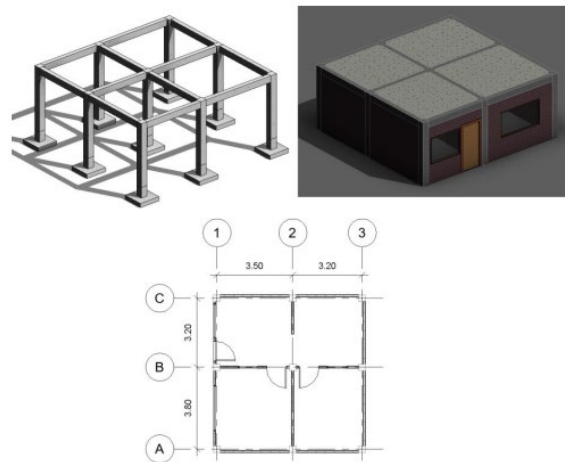


Figure 3. Schematic representation of M-PCP1-T1. Reprint from [1]

### Concrete Frames - 1 Story (M-PCP1-T2).

It is a one (1) story concrete frame structure, with a slender rectangular geometry in plan. Figure 4 shows a generic distribution of the structural elements of this building type. Its main characteristics are:

- Slim rectangular geometry in plan.
- Square columns (25cm x 25cm)
- Rectangular beams (25cm x 30cm)
- Mezzanine height of 3m.
- Concrete slab thickness 10cm.

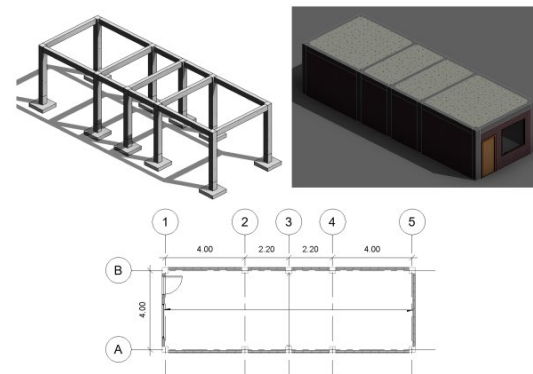


Figure 4. Schematic representation of M-PCP1-T2. Reprint from [1]

### Concrete frames - 2 stories (M-PCP2).

It is a concrete frame structure with two (2) floors, with a rectangular geometry in plan. Figure 5 shows a generic distribution of the structural elements of this building type. Its main characteristics are:

- Rectangular columns of 30cm wide.
- Rectangular beams (30cm x 40cm).
- Concrete slab for the upper level, light cover.
- Dividing walls and facades in masonry of clay blocks with a thickness of 12cm.
- Mezzanine height of 3m.
- Concrete slab thickness 10cm.

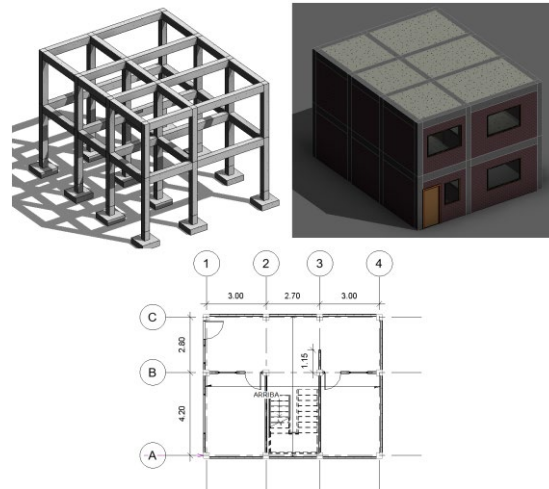


Figure 5. Schematic representation of M-PCP2. Reprint from [1]

### Concrete frames - 3 floors (M-PCP3).

It is a concrete frame structure is a structure with three (3) floors, with a slender geometry in plan. Figure 6 shows a generic distribution of the structural elements of this building type. Its main characteristics are:

- Rectangular columns of 35cm wide.
- Rectangular beams (30cm x 40cm).
- Dividing walls and facades in masonry of clay blocks with a thickness of 12cm.
- Mezzanine height of 3m.
- Concrete slab thickness 10cm.

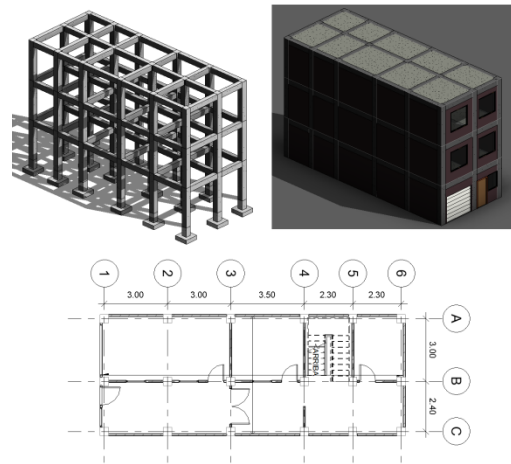


Figure 6. Schematic representation of M-PCP3. Reprint from [1]

The methodological workflow for their derivation is shown in Figure 7. It comprises computational nonlinear structural analysis using the finite element models for the six undamaged building prototypes previously shown to obtain their respective nonlinear structural capacities applying the OpenSees® platform [2]. Thereby, using a simplified Monte Carlo statistical algorithm, the demand tsunami forces are scattered over various flow velocities and momentum flux for an exhaustive set of tsunami inundation depth values. The average-inter-storey drift ratio proposed by HAZUS [4] was used to constrain four structural damage states and to fit the exceedance probabilities of the simulated data and generate their lognormal cumulative distribution functions in terms of inundation depth (m) as IM. Six properties were considered as random variables for a typical reinforced concrete building: the strength of the three construction materials involved ( $f'_c$ : concrete;  $f'_m$ : masonry; and  $f_y$ : steel), the tsunami force parameters of the drag coefficient (CD) and opening coefficient ( $C_o$ ), and the orientation of the building, representing the direction of the tsunami in relation to all of the building's possible orientations (0 to 360 degrees) [3].

The fragility functions  $F_{T_r^i, q_{N_i}}$  for a set of damage states for a set of building types  $T_r$ , and composed by a set of  $q_{N_i}$  damage limite states (for any hazard of interest  $i$ ), are assumed to be modeled by cumulative lognormal distributions. They are defined by their respective logarithmic means  $\mu_{q_0}(T_r^i)$  and their logarithmic standard deviations, for which we assume that their initial damage states  $q_{N_i}$  are all represented by a zero  $q_0$  (for a pristine, intact structure). The original values for the analytical tsunami fragility functions of the six building types proposed by Medina, 2019 are provided in Table 1.

In order to develop state-dependent fragility functions for such an existing model, we propose to use ad-hoc calibration parameters to modify these logarithmic mean values. For such a modification, we have to apply them the exponential operator to obtain the physically accountable mean IM (hazard intensity measures)  $\lambda_{q_0}(T_r^i)$  that define each damage state.

$$\lambda_{q_0}(T_r^i) = e^{\mu_{q_0}(T_r^i)}$$

For a set of damage states  $q_{N_i}$  in pristine structures, there is a corresponding set of values  $\lambda_{q_0} = [\lambda_{q_{01}}, \lambda_{q_y}, \lambda_{q_w}, \dots, \lambda_{q_{0i}}]$ . We propose to obtain their respective differences  $\Delta\lambda_{q_0}$ . For example:  $\Delta\lambda_{q_{01,2}} = \lambda_{q_{02}} - \lambda_{q_{01}}$  and  $\Delta\lambda_{q_{01,3}} = \lambda_{q_{03}} - \lambda_{q_{01}}$ . For the Medina, 2019 model that defines  $q_{N_i} = 4$ , there is a set of damage states  $\lambda_{q_0} = [\lambda_{q_{01}}, \lambda_{q_{02}}, \lambda_{q_{03}}, \dots, \lambda_{q_{0i}}]$  for which we obtain the differences between all the possible top and bottom damage states. Thus for this case, one must obtain six values:

$$\Delta\lambda_{q_0} = [\Delta\lambda_{q_{01,2}}, \Delta\lambda_{q_{01,3}}, \Delta\lambda_{q_{01,4}}, \Delta\lambda_{q_{02,3}}, \Delta\lambda_{q_{02,4}}, \Delta\lambda_{q_{03,4}}]$$

The  $\Delta\lambda_{q_0}$  of the Medina, 2019 model are reported in Table 2. The  $\Delta\lambda_{q_0}$  factors are proposed to be multiplied by their respective  $\lambda_{q_0}(T_r^i)$  and reframed the resulting quantity to a natural logarithm in order to approximate it back again to lognormal mean values. This is expressed as follows:

$$\delta_{w|y} = \ln((\Delta\lambda_{q_0})(\lambda_{q_0}))$$

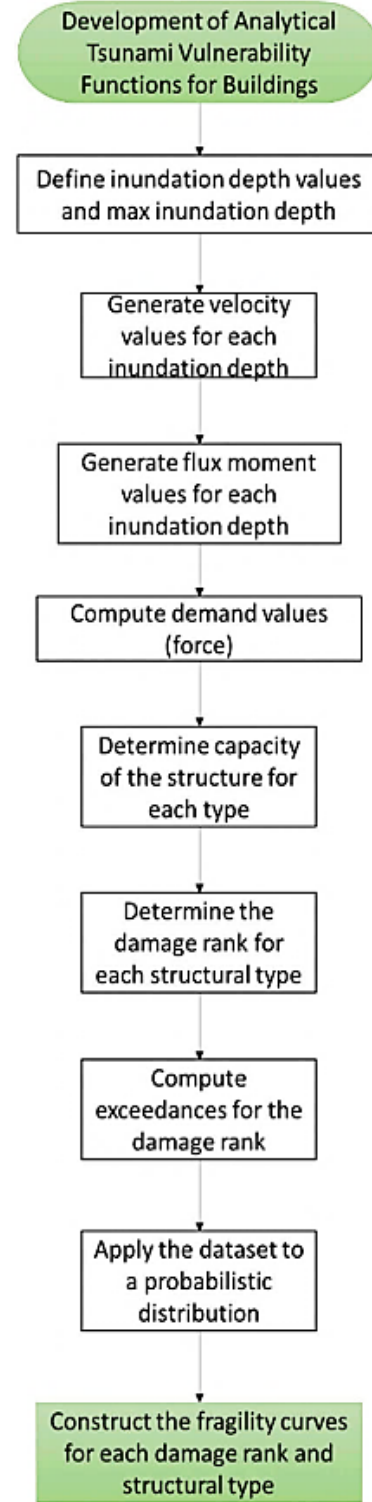


**Figure 7.** Workflow used to develop analytical tsunami fragility functions in [1] and [3]. Figure reprinted from [5].

In order to be consistent to the paper this repository is a supplement for, as well as with the approach proposed by Mignam et al, 2014 [6], we rename  $\Delta\lambda_{q_0}$  as  $\varphi$ . In the case more robust methods get available in the future to obtain transition probabilities (e.g. the use of sequential Monte-Carlo approaches with validation to address how some building components might change with time (due to diverse hazard sequences)), one could also obtain such a calibration parameters as follows:

$$\Delta\lambda_{q_0} = \varphi = e^{\delta_{wly}} / \lambda_{q_0}$$

The reader should note that in this approach, the  $\Delta\lambda_{q_0}$  are a set of ad-hoc calibration parameters that are applied directly to the IM  $\lambda_{q_0}$  for which each damage limit state was originally derived. These values form the lognormal mean of the state-dependent fragility functions. The corresponding values are reported in Table 3. Their standard deviations are assumed to be the same as the ones of the original model. An alternative (but still quite similar) approach is proposed by Mignam et al, 2014 [6].

**Table 1.** Original logarithmic mean and logarithmic standard deviations of the analytical tsunami fragility functions proposed by Medina, 2019 [1] for six building types.

Building type	D1 mean	D2 mean	D3 mean	D4 mean	D1 stddev	D2 stddev	D3 stddev	D4 stddev
M-MP	-0.655	-0.428	-0.386	-0.378	0.432	0.555	0.64	0.683
M-PCP1-T1	-0.103	0.248	0.416	0.533	0.282	0.303	0.338	0.37
M-PCP1-T2	-0.097	0.251	0.43	0.553	0.31	0.335	0.376	0.405
M-PCP2	0.432	0.767	0.92	1.004	0.267	0.3	0.353	0.385
M-PCP3	0.75	1.091	1.217	1.251	0.281	0.319	0.381	0.411
M-PN	-1.069	-0.511	-0.056	0.349	0.511	0.456	0.402	0.428

**Table 2.**  $\Delta\lambda_{q_0}$  or  $\varphi$  ad-hoc calibration parameters for the pairs of progressive damage states proposed herein for the Medina, 2019 [1] model.

Building type	D1-2	D1-3	D1-4	D2-3	D2-4	D3-4
M-MP	0.132	0.160	0.166	0.028	0.033	0.005
M-PCP1-T1	0.379	0.614	0.802	0.234	0.423	0.188
M-PCP1-T2	0.378	0.630	0.831	0.252	0.453	0.201
M-PCP2	0.613	0.969	1.189	0.356	0.576	0.220
M-PCP3	0.860	1.260	1.377	0.400	0.517	0.117
M-PN	0.257	0.602	1.074	0.346	0.818	0.472

**Table 3.** Resulting state-dependent logarithmic mean values for the pairs of progressive damage states proposed herein for the Medina, 2019 [1] model.

Building type	D1-2 mean	D1-3 mean	D1-4 mean	D2-3 mean	D2-4 mean	D3-4 mean
M-MP	-2.677	-2.486	-2.452	-4.005	-3.827	-5.596
M-PCP1-T1	-1.072	-0.591	-0.324	-1.203	-0.613	-1.255
M-PCP1-T2	-1.071	-0.560	-0.282	-1.128	-0.541	-1.173
M-PCP2	-0.057	0.400	0.605	-0.266	0.215	-0.595
M-PCP3	0.599	0.981	1.070	0.174	0.430	-0.930
M-PN	-2.429	-1.576	-0.997	-1.573	-0.712	-0.807

A Python script named “*AdHoc\_state\_dependent\_fragility\_Medina\_2019.py*” that handles the original input model (*Medina\_2019\_fragility.json*) and produces the state-dependent fragility model as outputs (*SDFF\_TS\_Medina\_et\_al\_2019*, in CSV and JSON formats). The JSON file is generated because it contains the metadata and specific data structure of the required by the software *Assetmaster* [7] and *DEUS* [8] for further physical vulnerability calculations (damage and loss forecast), as documented in the paper for which this repository is a supplement. Complementary, a Python script named “*plot\_SDFF\_Medina\_2019.py*” can be used to reproduce the associated graphical representation of those new sets of state-dependent fragility functions, which are presented in the associated paper to this repository.

## 5. Acknowledgments

These models have been constructed within the framework of the RIESGOS and RIESGOS 2.0 projects, funded by the German Federal Ministry of Education and Research (BMBF), with Grant No. 03G0876A-J and 03G0905A-H, respectively. These projects are part of the funding programme CLIENT II – International Partnerships for Sustainable Innovations’. We greatly thank Cecilia Nievas, Fabrice Cotton, Massimiliano Pittore and Juan Páez-Ramírez for their constructive feedback.

## 6. References

- [1] Medina, S.: Zonificación de la vulnerabilidad física para edificaciones típicas en San Andrés de Tumaco, Costa Pacífica Colombiana, Universidad Nacional de Colombia Facultad de Ingeniería, Departamento Ingeniería Civil y Ambiental, 2019. <https://repositorio.unal.edu.co/handle/unal/77178>
- [2] McKenna, F.; Fenves, G.L. Scott, M.H.: Open system for earthquake engineering simulation (OPEENSEES), Pacific Earthquake Engineering Research Center; 2000, Available: <http://opensees.berkeley.edu/>
- [3] Medina, S.; Lizarazo-Marriaga, J.; Estrada, M.; Koshimura, S.; Mas, E.; Adriano, B.: Tsunami analytical fragility curves for the Colombian Pacific coast: A reinforced concrete building example, *Engineering Structures*. 196 (2019) 109309. <https://doi.org/10.1016/j.engstruct.2019.109309>
- [4] FEMA, HAZUS-MH MR3 earthquake model technical manual, Federal Emergency Management Agency, Washington, D.C., 2008.
- [5] Paez-Ramirez, J. Lizarazo-Marriaga, J.; Medina, S.; Estrada, M.; Mas, E. Koshimura, S.: A comparative study of empirical and analytical fragility functions for the assessment of tsunami building damage in Tumaco, Colombia, *Coastal Engineering Journal*. 62 (2020) 362–372. <https://doi.org/10.1080/21664250.2020.1726558>
- [6] Mignan, A.; Wiemer, S.; Giardini, D.: The quantification of low-probability–high-consequences events: part I. A generic multi-risk approach, *Natural Hazards*. 73 (2014) 1999–2022. <https://doi.org/10.1007/s11069-014-1178-4>
- [7] Pittore, M., Gomez-Zapata, J. C., Brinckmann, N., & Rüster, M.: *Assetmaster* and *Modelprop*: web services to serve building exposure models and fragility functions for physical vulnerability to natural-hazards. V. 1.0, GFZ Data Services. (2021). <https://doi.org/10.5880/riesgos.2021.005>
- [8] Brinckmann, N., Gomez-Zapata, J. C., Pittore, M., & Rüster, M.: *DEUS*: Damage-Exposure-Update-Service. V. 1.0., GFZ Data Services. (2021). <https://doi.org/10.5880/riesgos.2021.011>